SSRG International Journal of Electrical and Electronics Engineering
ISSN: 2348-8379/ https://doi.org/10.14445/23488379/IJEEE-V13I4P106

Volume 13 Issue 4, 77-96, April 2026

Original Article

Analysis of DC-DC Converters for Induction Heating Application

B. Harshini[1], Naga Swetha. B[2], N. Krishna Kumari[3]

[1,2,3] *Department of Electrical and Electronics Engineering, VNR Vignana Jyothi Institute of Engineering and Technology, Hyderabad, Telangana, India.*

[1]*Corresponding Author : brhu.hcb@gmail.com*

Received: 12 January 2026 Revised: 22 February 2026 Accepted: 22 March 2026 Published: 30 April 2026

Abstract *- Nowadays, power converters are becoming crucial in the usage of renewable energy sources. In this paper, three diverse DC-DC converters have been discussed, which provide high gain with fewer components and are economical. Using MATLAB/Simulink, these three different topologies have been compared in terms of gain and Total Harmonic Distortion (THD) using various sources of energy. The topologies are incorporated with only one switch the losses can be reduced. The findings indicate that DC-DC Converters with an input voltage of 48V are thought to attain up to a gain of about 10 when compared with other topologies. With this, numerous high-gain DC-DC converters are being extended to induction heating applications. Furthermore, THD of 0.5% or less is guaranteed by the recommended topology. And also, these DC-DC Converters are mostly utilized in Electric Vehicles (EVs) and Uninterruptible Power Supply (UPS). Additionally, their small size, controllability, and increased efficiency make them appropriate for integration with high-frequency inverters, smart home energy interfaces, and microgrid systems that rely on renewable energy sources. According to simulation results, the converter's dynamic performance and stability make it dependable for use in both residential and commercial energy applications. They are appropriate for grid-connected applications and next-generation smart energy systems due to their straightforward control mechanism, scalability, and excellent performance under dynamic load conditions.*

Keywords *- DC-DC Converters, Induction Heating (IH), Non-Isolated, Total Harmonic Distortion (THD), Voltage Gain.*

1. Introduction

In this integration of a PV system into a microgrid, it is possible with dual capacitors, dual diodes, and a single switch DC-DC Boost converter has been designed, thereby minimizing switching and stray losses, which is advantageous. The performance has been compared in terms of gain and with step response, also [1]. To achieve low ripple, High Voltage (HV) gain, minimized switch stress, and low converter costs, research has been focused on modifying traditional power converters with High Gain DC-DC Converters (HGDCC) using PV systems, and HGDCC has been utilized in motor drive applications [2]. In this, a non-isolated non-coupled inductor-based HGDCC has been proposed that has merits over the other topologies, such as HV gain at lower duty cycle and Low Voltage (LV) stress on controlled power switches, which leads to lighter, more flexible management, more compact, and less expensive. Moreover, this HGDCC performance has been compared with various other developed topologies [3].

In this, an HGDCC has been compared with two switches and Voltage Multiplier Circuits (VMC) in terms of gain, efficiency, fewer components, and THD for IH application [4]. The Hybrid Energy Storage Systems (HESS) are capable of fully utilizing the high power density of Supercapacitors (SCs) and the high energy density of batteries to improve the dynamic performance and energy efficiency of EVs. In the MATLAB Simulink environment, the EVs' performance was studied during transient modes [5]. A Hybrid Energy System (HES) uses a different energy source with variation in voltage-current characteristic, such as solar, wind, fuel cells, batteries, SCs, etc. In this, a multi-input DC-DC converter has been used with a power electronic interface and integrates with these energy sources. A two-input DC-DC converter topology has been proposed, which has achieved high gain, with fewer components, without the need for a VM cell or any circuit, when compared with the current converter [6]. Compared to contemporary boost converters, a smaller circuit with a single switch and fewer passive parts has been created. These have low switching losses and are operated effectively for HV gain at a low duty cycle. And also to increase the voltage, the number of additional cells can be connected in cascade [7]. For IH applications, resonant inverters with energy dosing are suggested. These power topologies differ in that the DC power source's power consumption is determined by the operating frequency, the resonant capacitor's value, and the DC supply voltage rather than the load's size and fluctuations [8]. For Fuel Cell Electric Vehicles (FCEVs), a DC-DC converter with a high conversion ratio has been proposed. This paper suggests a fuel cell-based non-isolated high-gain integrated DC-DC converter for EVs. This topology, which includes an Interleaved Boost Converter (IBC), coupled inductors, a switched capacitor cell, a passive clamp circuit, and VMC at the source end, produces a smooth, ripple-free input current and a voltage gain of 12.33 at a lower duty ratio of 0.45. Additionally, the Fuzzy Logic Controller (FLC) -based Maximum Power Point Tracking (MPPT) controller and the suggested Radial Basis Function Network (RBFN) MPPT technique are contrasted. As demonstrated by the simulation and hardware results, the RBFN-based MPPT controller outperformed the FL -based controller in tracking the maximum power [9]. A new DC-DC converter that works in boost converter mode, mainly based on a Single-Ended Primary Inductance Converter. The converter's design has been modeled with a Quasi-Z Source (QZS) structure and Switched Capacitor (SC) cell to increase the gain of the system. By proper tuning of the Proportional Integral (PI) controller, the converter attained an efficiency of 92% and a gain of about 12 [10]. The traditional ZS network with SC cells that propose three high step-up ZS based dc–dc converters. This converter has a straightforward design with low voltage stress on semiconductor devices, high voltage gain, and a smooth input current. Furthermore, the suggested converters do not place any restrictions on the power switch's duty cycle, in contrast to certain ZS-based topologies that are now used. Because of these features, the suggested converters are great options for connecting a high-voltage DC bus to an LV Solar Photovoltaic (PV) panel in PV applications [11]. In this, a new transformer-less single switch HGDCC for Renewable Energy Systems (RES) has been introduced. This converter solves two main problems in order to raise the PV panel's voltage and provide a constant input current: the low voltage generated by PV solar panels and the intermittent input current brought on by switching power supplies. A VMC and a switched capacitor/inductor cell are added to the conventional boost converter to create the suggested converter in order to enhance the gain and minimize the stress on the power devices [12]. An isolated multilevel bidirectional Dc–Dc converter has been proposed to connect the LV battery and HV propulsion inverter in EVs. This topology achieves an HV step-up ratio in the motoring mode by rearranging two split-capacitor half-bridge circuits in series/parallel with a two-quadrant switch. During regenerative braking, the converter utilizes phase shift modulation between the LV full bridge and the HV half bridges in order to control the battery voltage. For a wide load range, the full-bridge devices achieve zero voltage switching by various modulation strategies [13]. Because of its merits, such as quick heating times, increased control, and efficiency, IH is currently utilized in homes. Conduction and switching loss, a comparatively high component count and cost, the need for an additional DC link capacitor, an electromagnetic compatibility filter, and other issues are some of the main disadvantages of conventional design. The direct Ac-Ac half bridge boost converter, which is comparable to a half bridge series resonant inverter and a synchronous boost Dc-Dc converter, is a novel topology for applications involving IH in homes [14]. When compared to conventional boost DC-DC converters, a ZS boost DC-DC converter and a Multilevel Inverter (MI) have been considered; the modified converter with the conventional ZS network has HV gain. The source and converter are connected by an impedance network, which serves as a bridge that doesn't require any additional parts. Modified converter size and cost are decreased, and efficiency is improved due to less voltage stress experienced by the switches and diodes, rather than conventional boost DC converters. A multilevel output voltage is produced by the MI with a split DC link and a bidirectional switch [15]. An HGDCC is proposed for a variable speed AC drive application. A generalized synchronous rotating reference frame is used to model the induction machine. Conventional Sine Pulse Width Modulation (SPWM) and Space Vector Pulse Width Modulation (SVPWM) techniques are used to generate the pulses for a three-phase inverter [16]. Using coupled inductors and with many components (4 diodes, 6 capacitors), trying to achieve high gain from the converter topology [17].

For the IH application series, resonant inverters are mostly used to obtain High-Frequency (HF) current. An HF transformer is used to match the voltage and current of the inverter [18]. The need for effective power conversion systems has been highlighted by the rising demand for sustainable energy sources like fuel cells and Photovoltaic (PV) systems. For many high-power applications, including DC microgrids, motor drives, and energy storage systems, these sources usually generate low DC voltages that are insufficient. In order to raise these low input voltages to the necessary high-voltage DC bus levels, high-gain DC-DC converters are crucial as an interface. Although the structure of conventional DC-DC boost converters is straightforward, they have serious drawbacks when high voltage gain is needed. They must operate at extreme duty cycles in order to achieve a high step-up ratio, which causes a number of issues, including increased conduction losses, high voltage stress across the power switches and diodes, serious reverse-recovery problems in the diodes, and overall decreased efficiency. This work suggests a few high-gain topologies to overcome the drawbacks of traditional converters.

2. System Description

Figure 1 tells us that the various DC-DC converters have been considered with fewer components, such as a switch, a diode, and passive components, and fed to the load, where their gain and efficiency will be addressed. Moreover, Figure 2 discusses high-gain converters fed to an IH load using various sources such as a DC source, a battery, and an Ultra-Capacitor (UC), where its THD is addressed with various energy sources and converter topologies.

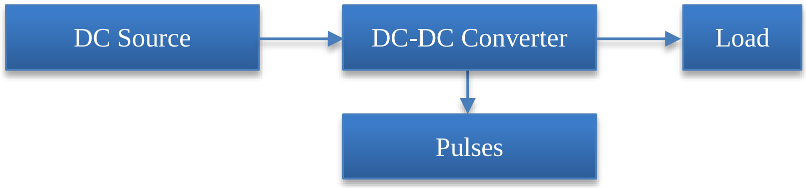

Fig. 1 Block Diagram for DC-DC Converters

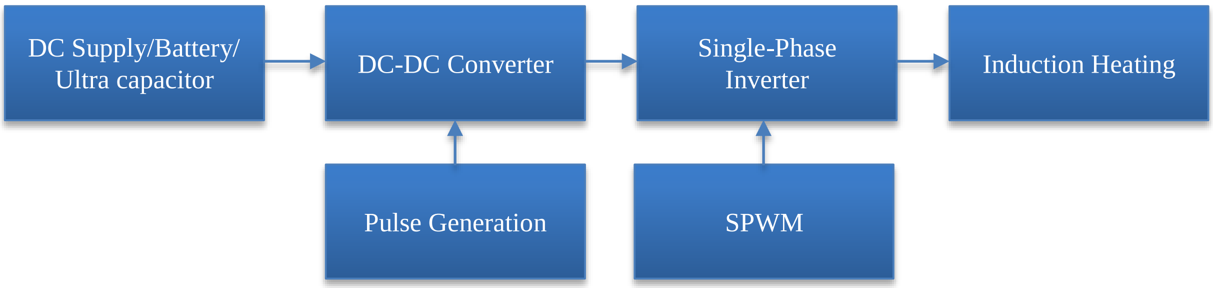

Fig. 2 Block Diagram for DC-DC Converters fed an IH load

2.1. High Gain DC-DC Converters (HGDCC)

HGDCC is shown in Figure 3, which has one MOSFET switch, one source of energy, two diodes, one inductor, two capacitors, and a load. HGDCC operates in two modes, i.e., when the switch is in the ON state and in the OFF state. When switch M is in the ON state, the diodes D1 and D2 are Reverse Biased (R.B.), and inductor L1 gets charged, and capacitors serve the load. When switch M is in the OFF state, the diodes D1 and D2 are Forward Biased (F.B.), and inductor L1 releases its energy, and capacitors serve the load. This HGDCC is further integrated with a single-phase inverter and used for an IH load, as depicted in Figure 4. For the positive half cycle, Sa, Sb are conducted, while for the negative cycle Sc, Sd are turned ON.

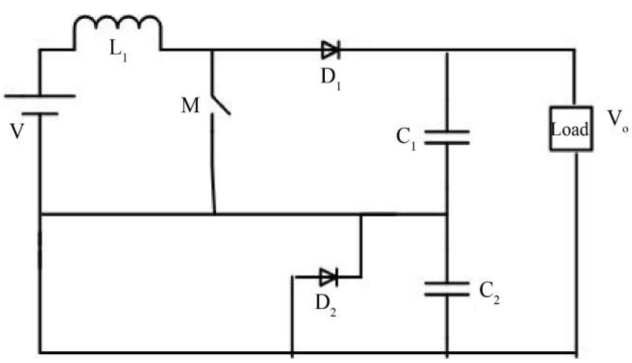

Fig. 3 HGDCC [1]

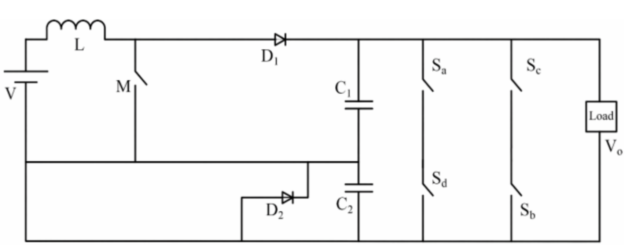

Fig. 4 HGDCC fed IH load

2.2. High Gain Cell DC-DC Converters (HGCDCC)

HGCDCC comprises a single source of energy, one MOSFET switch, three inductors, five diodes, and five capacitors, which is represented by Figure 5. HGCDCC operates in two modes, i.e., when the switch is in the ON state and when the switch is in the OFF state. When the switch is ON, diodes D1 and D2 are Reverse-Biased because of a negative Voltage VC across them. Consequently, output Capacitor C0 and the load are currently being charged by the series capacitor C. When the switch is turned OFF, then diodes D1 and D2 F.B. instantly allow inductor current to flow through, and negative voltage makes diode D3 R.B. This HGCDCC is further integrated with a single-phase inverter and used for an IH load, as depicted in Figure 6. For the positive half cycle, Sa and Sb are switched ON, while for the negative cycle, Sc and Sd are turned ON.

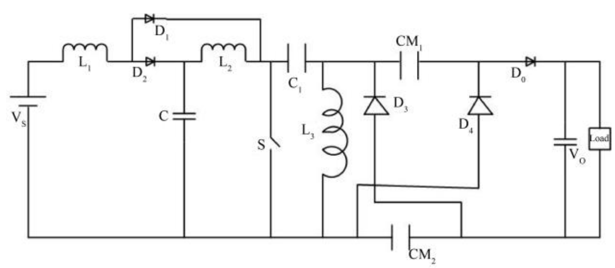

Fig. 5 HGCDCC [2]

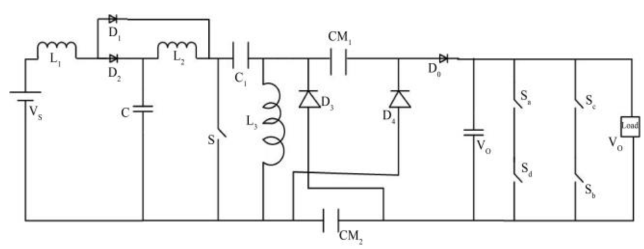

Fig. 6 HGCDCC fed IH load

2.3. Ultra High Gain DC-DC Converter (UHGDCC)

Proposed UHGDCC comprises a single source of energy, two MOSFET switches, three inductors L1 and L2, three diodes D1, D2, and D3, and three capacitors C1, C2, and C3, as shown in Figure 7. Both switches are operated by the same PWM signal. UHGCDCC operates in two modes, i.e., when switches are in the ON state and when switches are in the OFF state. When switches are ON, diodes D1 and D3 are R.B., and diode D2 is F.B. Energy moves from one source to both inductors, raising the current flowing through them. When switches turn off, then diodes D1 and D3 F.B., and diode D2 is R.B., the load receives energy that is stored in the converter's passive components. This UHGDCC is further integrated with a single-phase inverter and used for an IH load, as represented in Figure 8. For the positive half cycle, Sa and Sb are conducted, while for the negative cycle, Sc and Sd are switched ON. Table 1 displays the number of components in the recommended architecture in comparison to the HGDCC and HGCDCC. Table 2 displays the recommended topologies specifications, Table 3 and Table 4 indicate the specifications of the Battery and Ultracapacitor as a source of energy for the IH load.

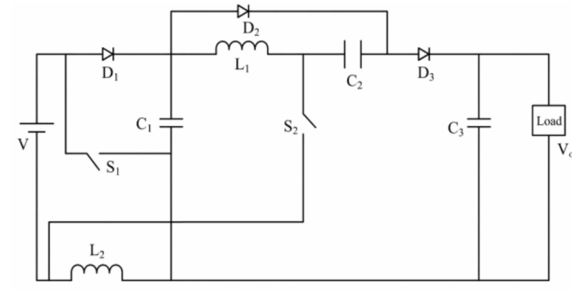

Fig. 7 UHGCDCC [3]

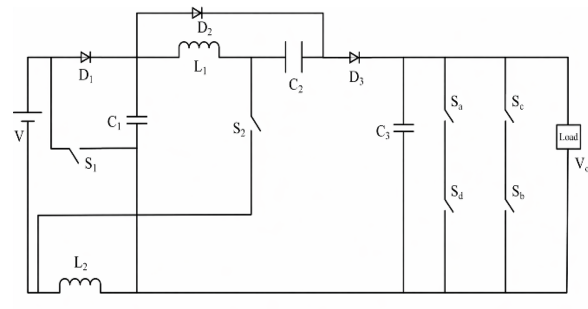

Fig. 8 UHGCDCC fed IH load

Table 1. Comparison Between the Number of Components Used in HGDCC, HGCDCC, and UHGDCC with the existing high-gain converters

Components	HGDCC	HGCDCC	UHGDCC	HGDCDCC [4]	Two-cell boost converter [7]	DC-DC Converter [19]
DC source	1	1	1	2	1	1
MOSFETs	1	1	2	3	1	1
Inductors	1	3	2	3	2	3
Capacitors	2	5	3	1	3	4
Diodes	2	5	3	1	4	6
Inverter switches	4	4	4	4	-	-

Table 2. Specifications

Parameter	Value
Voltage Source (V)	48V
Inductors (L1,L2)	24.5µH, 1mH
Capacitors (C1,C2,C3)	470µF
Load Resistance (RL)	62.5Ω
Load Inductance (LL)	7.2µH
Switching frequency (fs)	25kHz

Table 3. Battery Specifications

Parameter	Value
Rated Voltage (V)	48
Rated Capacity (Ah)	5.4
Initial SOC	100%

Table 4. Ultracapacitor Specifications [4]

Parameter	Value
Rated Voltage (V)	48V
Rated Farad (F)	15F
Initial Voltage (V)	46V

3. Results and Discussion

The outcomes for various topologies are as follows:

3.1. HGDCC

A single-input high-gain topology is used to raise the voltage from a single input source and achieve an intended output. The simulation circuit for the HGDCC converter is shown in Figure 9. The gate signals for the switch with a duty cycle of 40% are displayed in Figure 10. It can be observed that the switch is turned ON for 40% of the time period and for the remaining time it is in the OFF state. Gain can be found with the help of Figure 11, which displays the input and output voltage as well as the output current. It can be seen from the first plot that the input voltage is 48V, the output voltage is 90V, and the output current is 0.9A.

HGDCC topology is extended to IH load using various sources such as DC voltage source, Battery, and Ultracapacitor. Using these various sources, load voltage, load current, and its THD will be discussed.

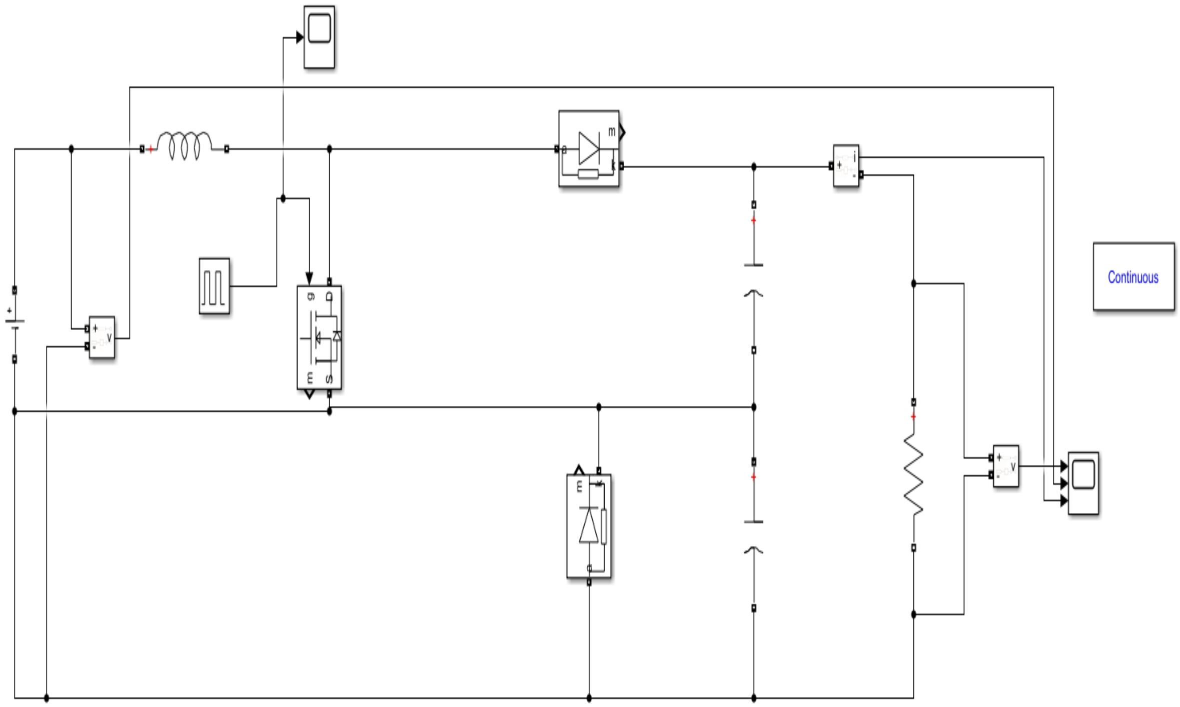

Fig. 9 Simulation Diagram of HGDCC

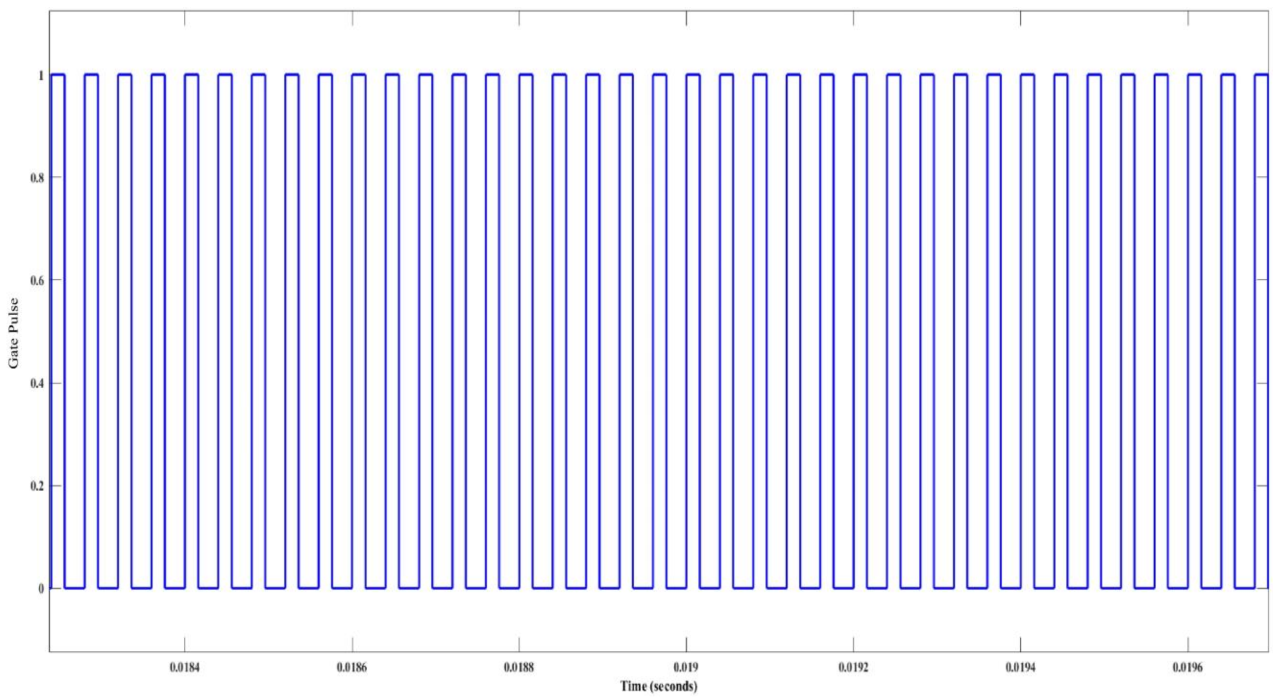

Fig. 10 Switch gate pulse

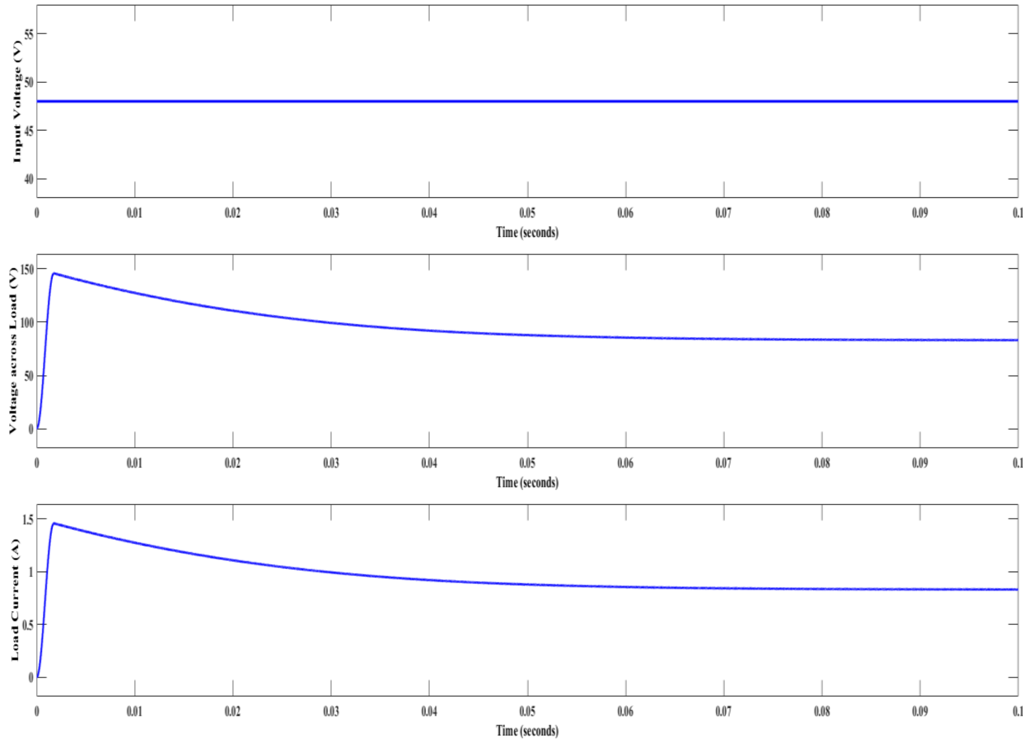

Fig. 11 Input Voltage, Output Voltage, and Load Current

3.1.1. HGDCC using DC Source

In the case of HGDCC for IH load using DC voltage source, the simulation diagram is shown in Figure 12, and the output voltage and output current of an IH load are plotted in Figure 13. THD of load voltage is discussed in Figure 14.

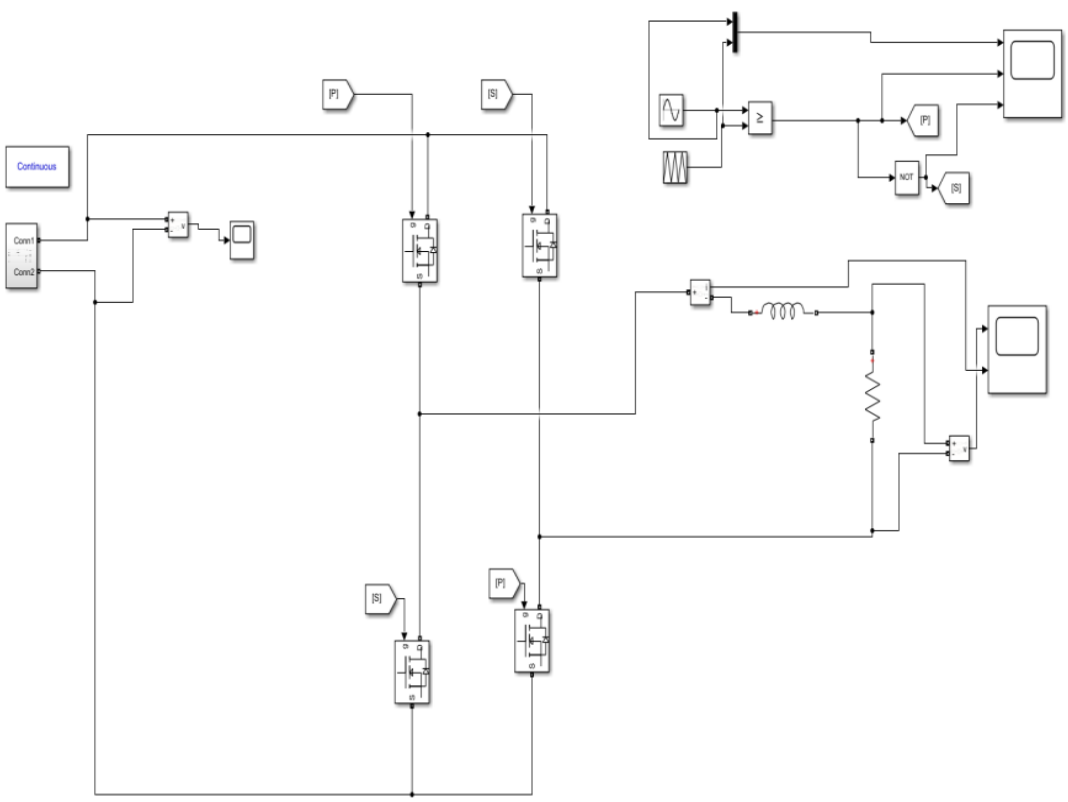

Fig. 12 Simulation Diagram of HGDCC using DC Source

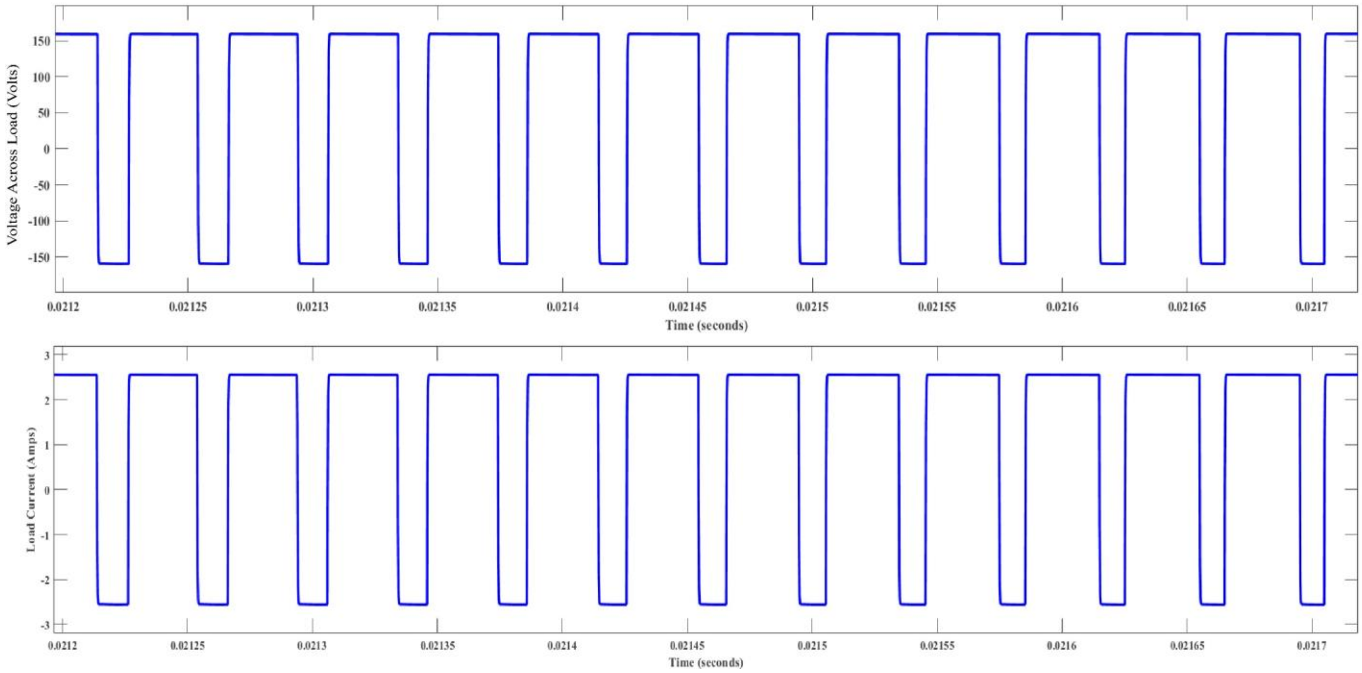

Fig. 13 Output Voltage and Output Current of the IH load

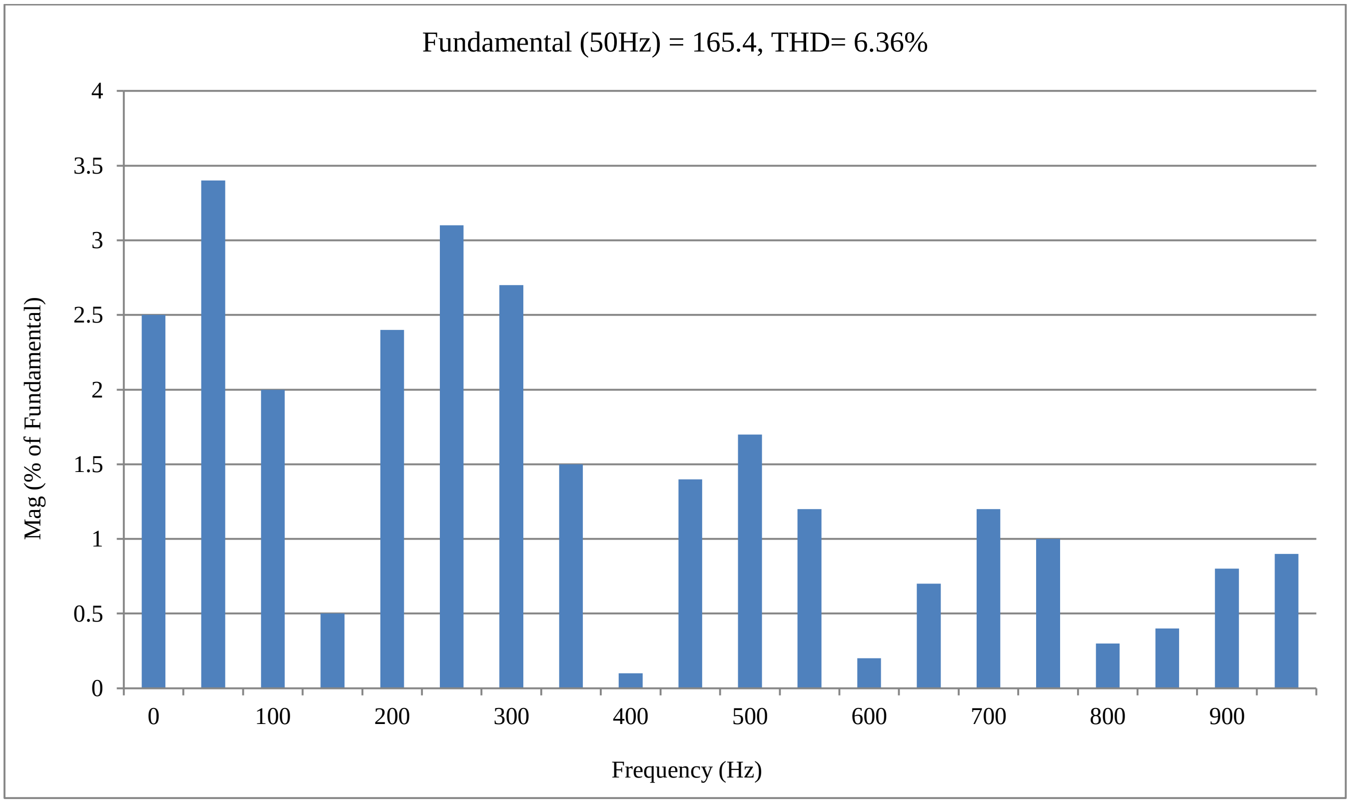

Fig. 14 Load voltage's THD using DC source

3.1.2. HGDCC using Battery as a source:

In the case of HGDCC for IH load using Battery, the simulation diagram is shown in Figure 15, and the output voltage and output current of IH load are described in Figure 16. THD of load voltage is shown in Figure 17.

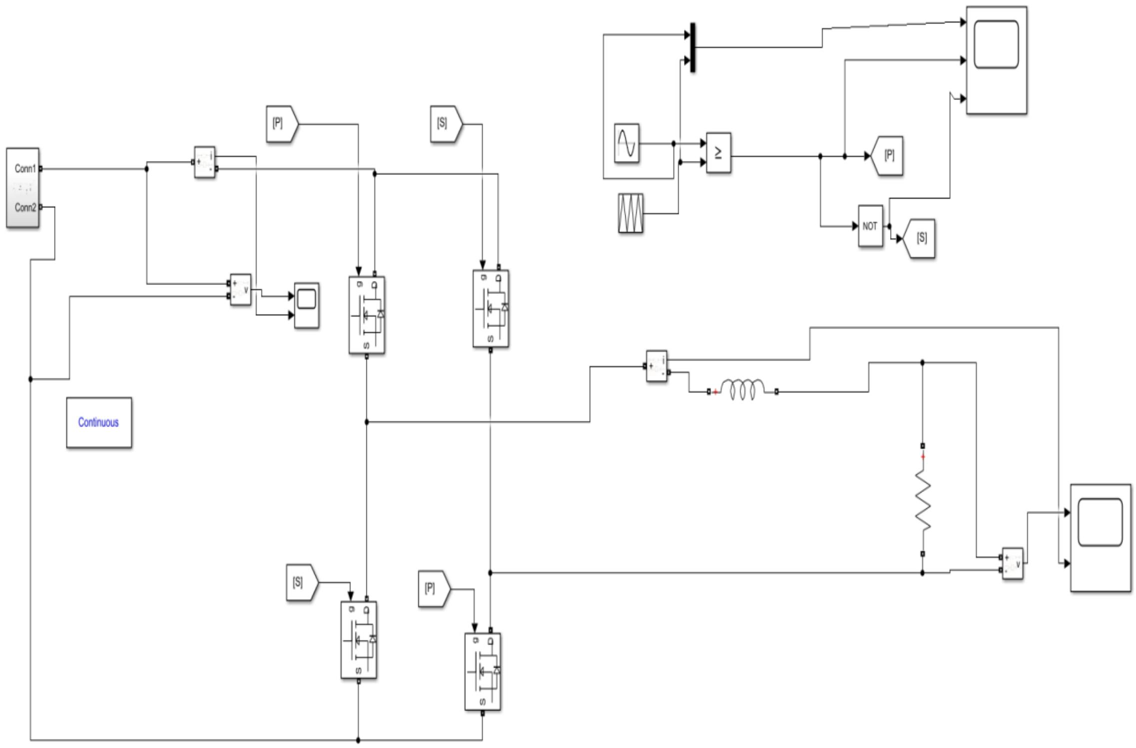

Fig. 15 Simulation Diagram of HGDCC using Battery as a Source

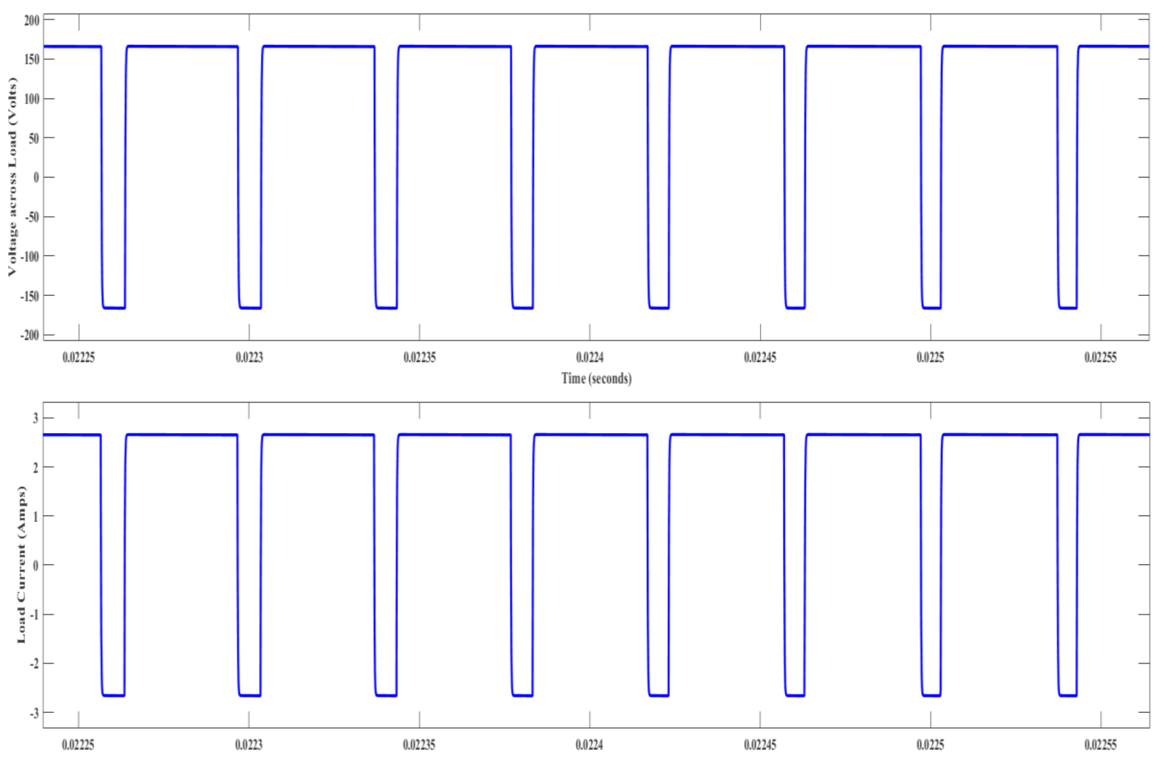

Fig. 16 Output Voltage and Output current of the IH load

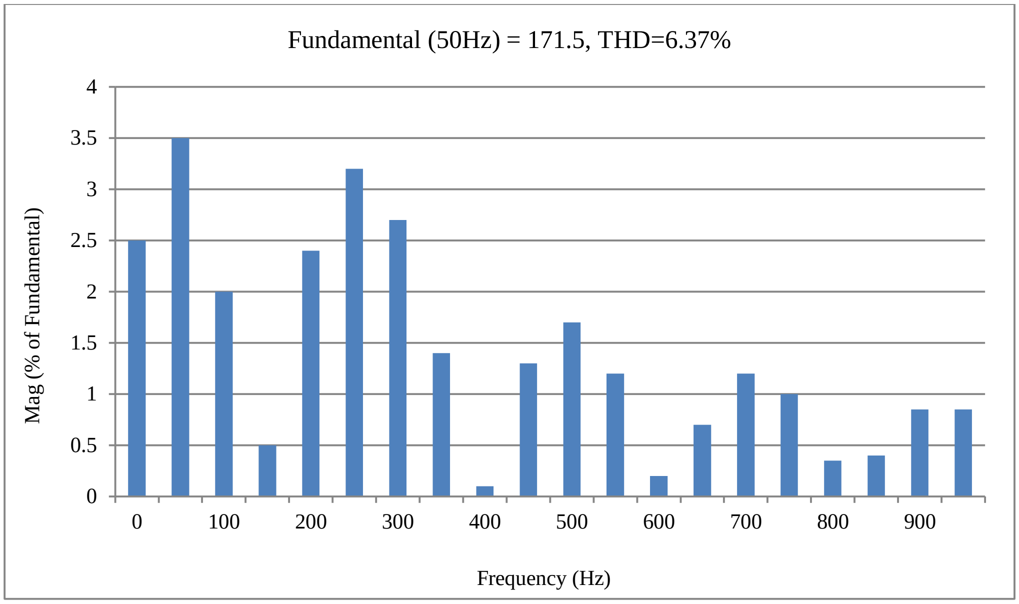

Fig. 17 Load voltage's THD using Battery

3.1.3. HGDCC using Ultracapacitor as a source

In the case of HGDCC for IH load using Ultracapacitor, its simulation diagram is depicted in Figure 18.

Figure 19 tells us about the output voltage and output current of an IH load. THD of the load voltage is shown in Figure 20.

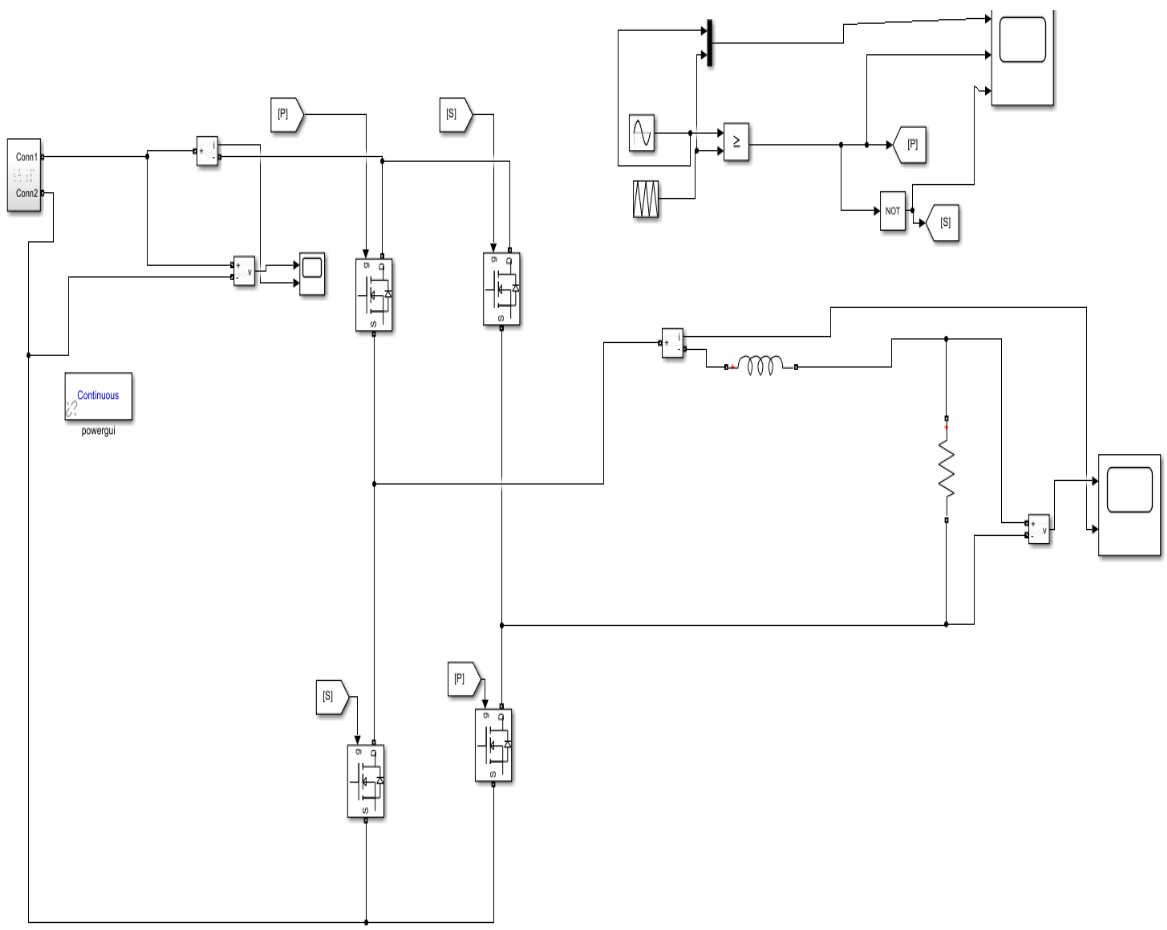

Fig. 18 Simulation Diagram of HGDCC using Ultracapacitor as a Source

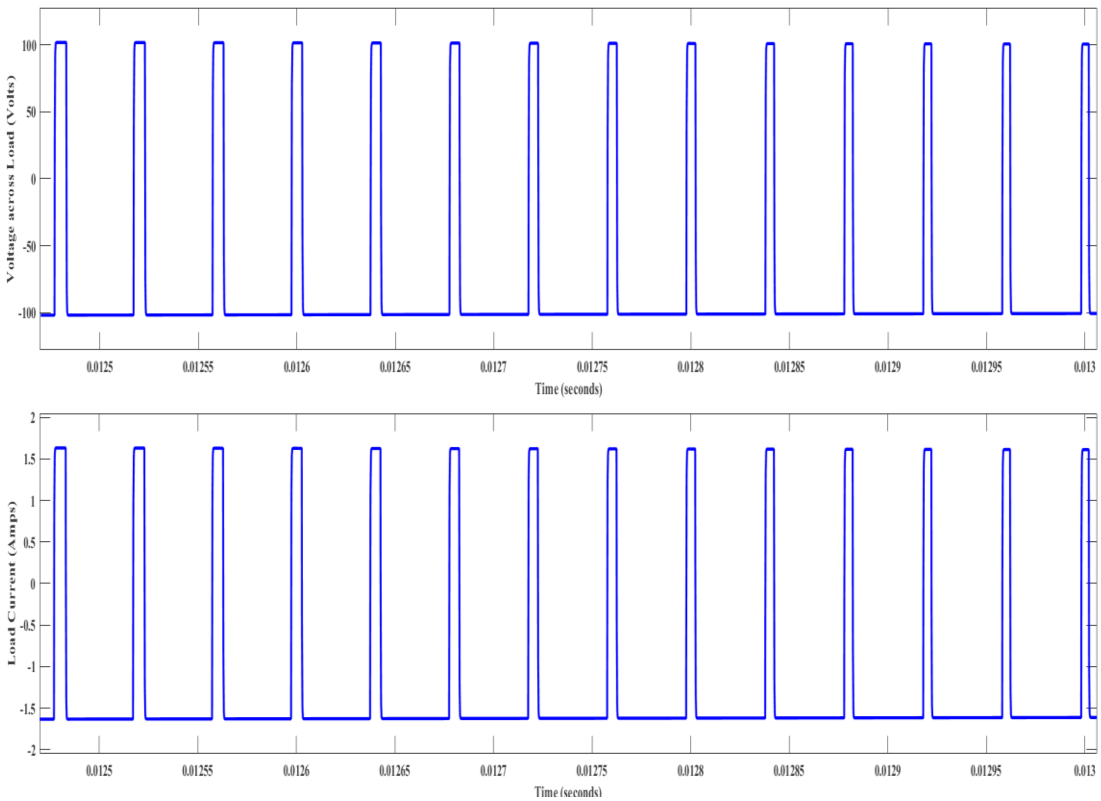

Fig. 19 Output Voltage and Output Current of the IH load

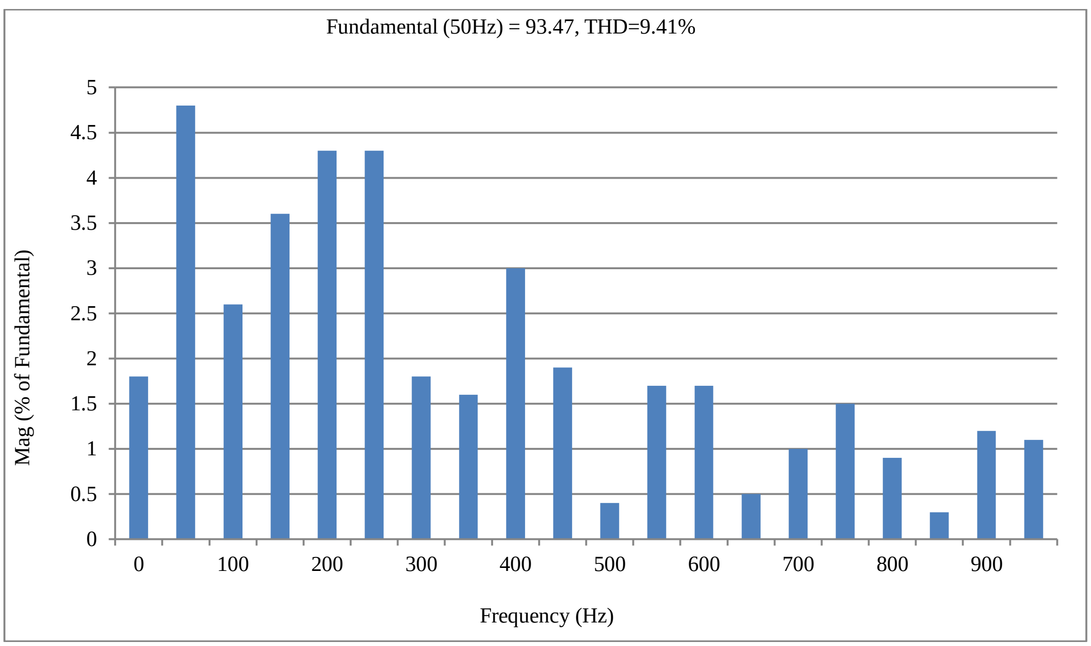

Fig. 20 Load voltage's THD using Ultracapacitor

3.2. HGCDCC

A single input with a single switch M using a high-gain cell achieves high gain from this topology. The simulation diagram is depicted in Figure 21. The gate signals for the switch with a duty ratio of 40%, which tells us that for 40% of the period the switch is in the ON state and for the rest of the time it is in the OFF state, as shown in Figure 22. Gain can be found with the help of Figure 23, which displays input and output voltage and output current, where the input voltage is 48V, the voltage across the load is 200V, and the load current is 2A.

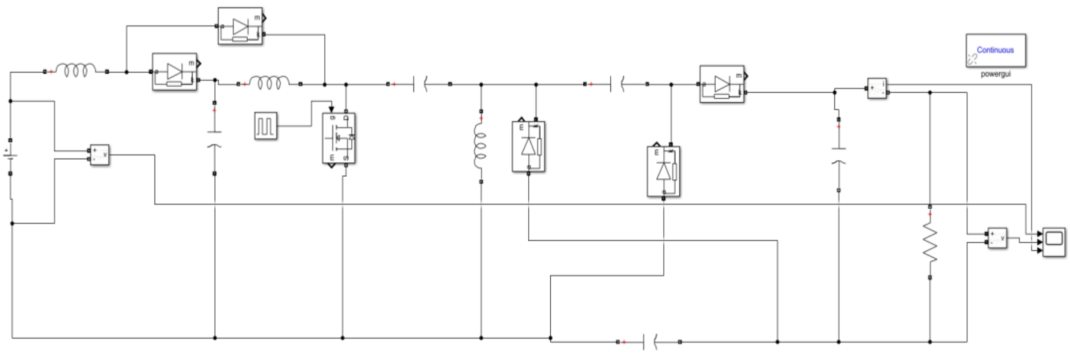

Fig. 21 Simulation Diagram of HGCDCC

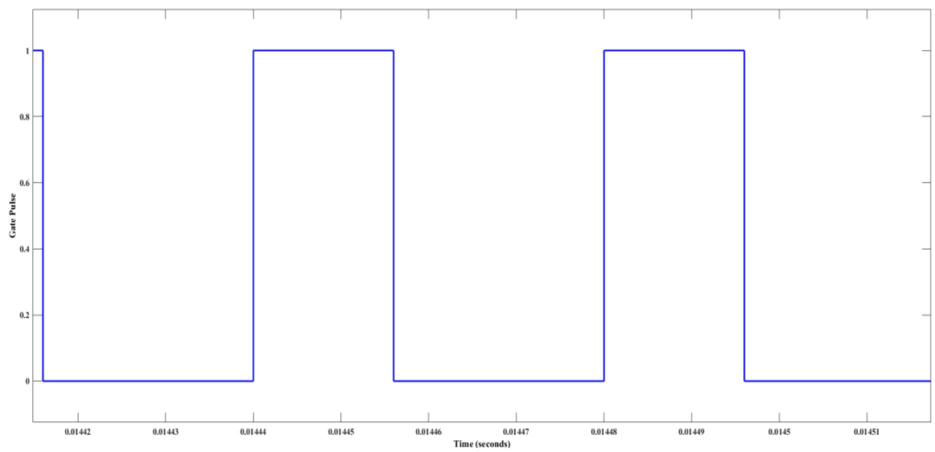

Fig. 22 Switch gate pulse

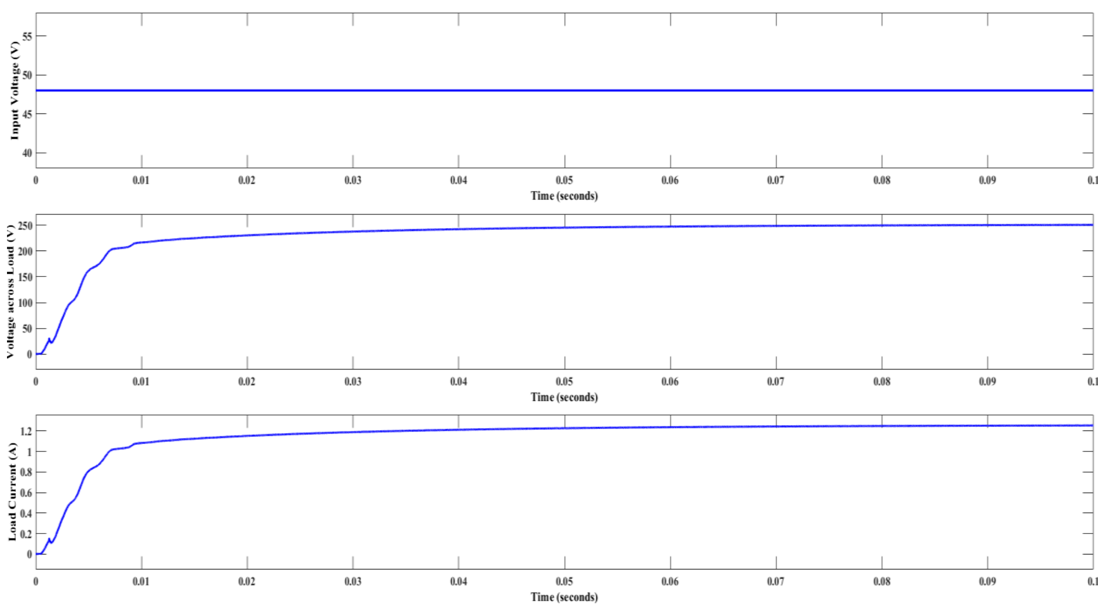

Fig. 23 Input Voltage, Output Voltage, and Load Current

3.2.1. HGCDCC using DC as a source

For HGCDCC for IH load using DC voltage source, the simulation circuit is shown in Figure 24.

Figure 25 shows a plot of the IH load's output voltage and output current. Figure 26 discusses the load voltage's THD.

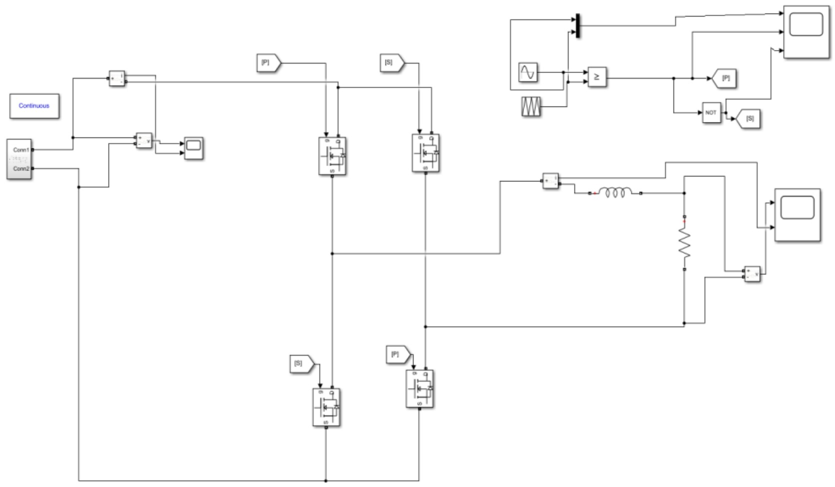

Fig. 24 Simulation Diagram of HGCDCC using DC Source

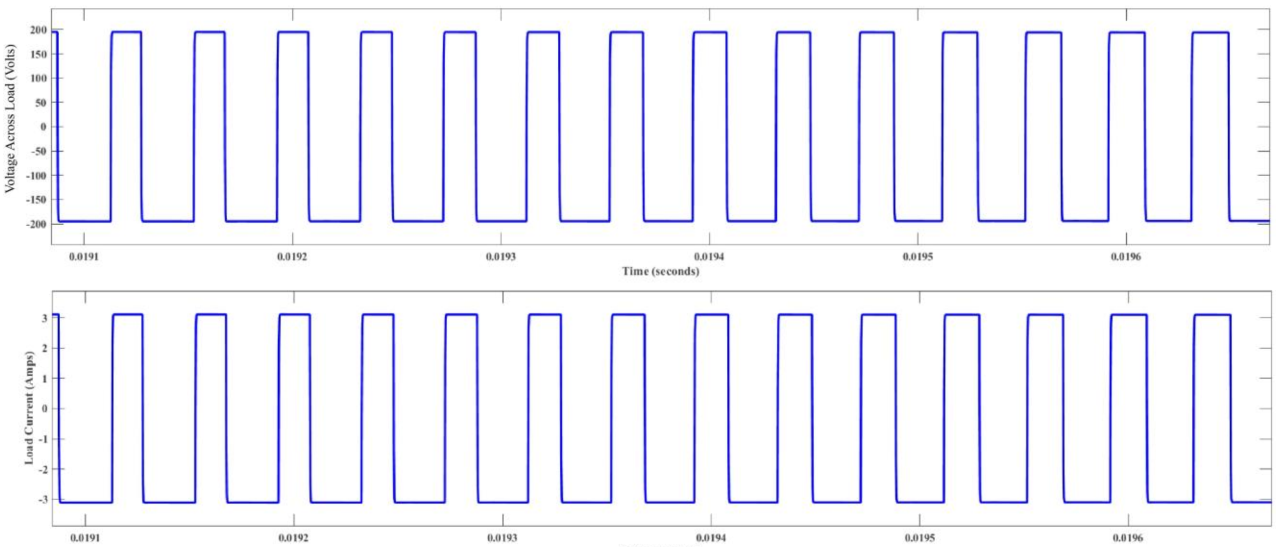

Fig. 25 Output Voltage and Output Current of the IH load

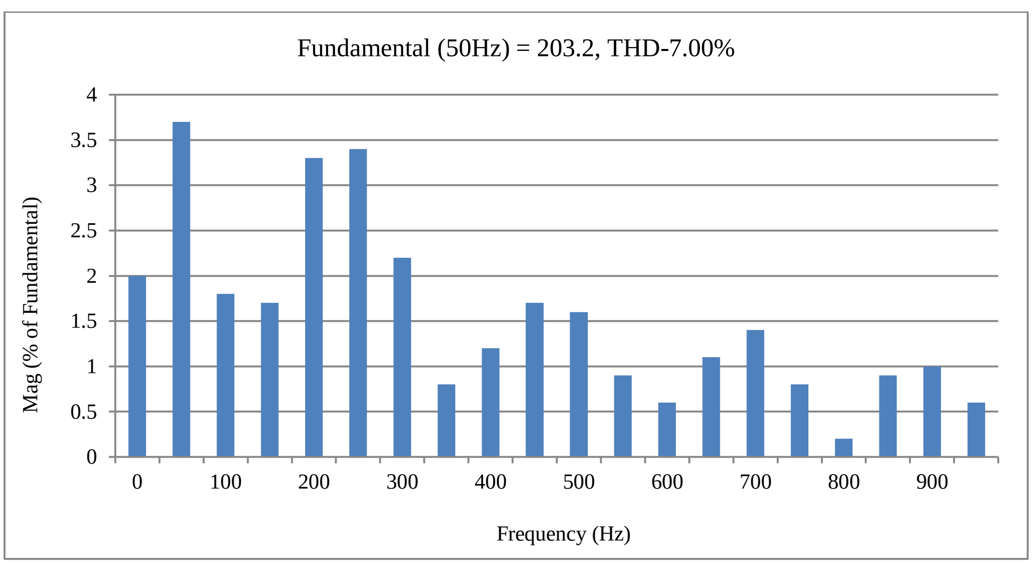

Fig. 26 Load voltage's THD using DC source

3.2.2. HGCDCC using Battery as a source:

For HGCDCC for IH load, using Battery, Figure 27 depicts the simulation circuit of HGCDCC.

Figure 28 represents an IH output voltage and output current. Figure 29 represents the load voltage's THD.

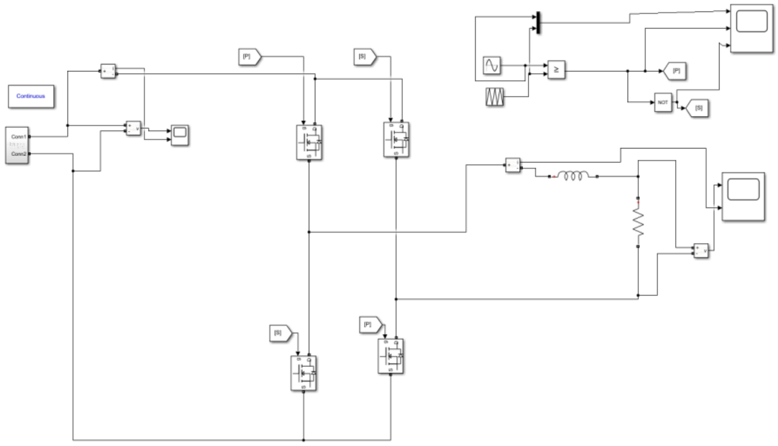

Fig. 27 Simulation Diagram of HGCDCC using Battery as a Source

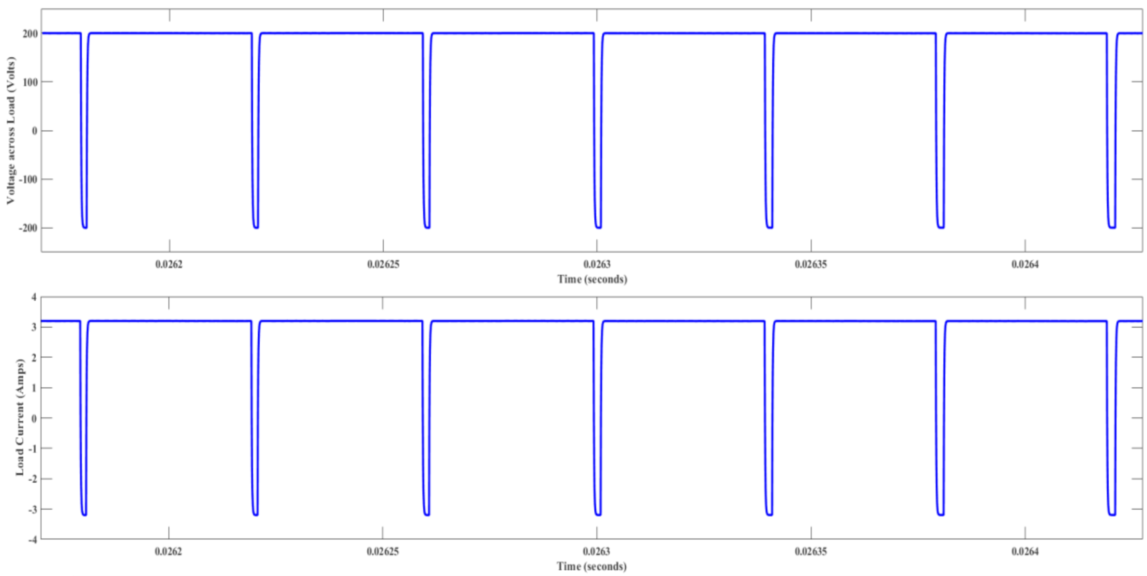

Fig. 28 Output Voltage and Output Current of the IH load

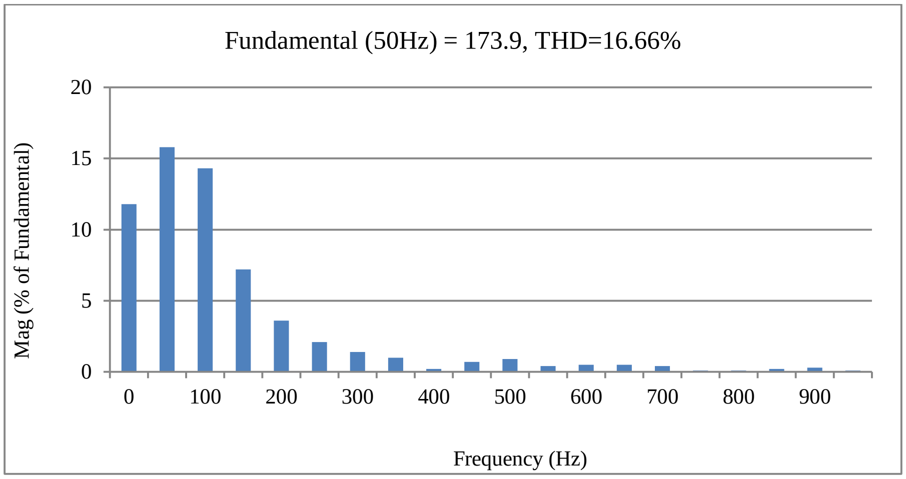

Fig. 29 Load voltage's THD using Battery

3.3.2. HGCDCC using Ultracapacitor as a source

For HGCDCC for IH load using Ultracapacitor, the simulation diagram is described in Figure 30, and its output voltage and output current of an IH load are described in Figure 31. THD of the load voltage is shown in Figure 32.

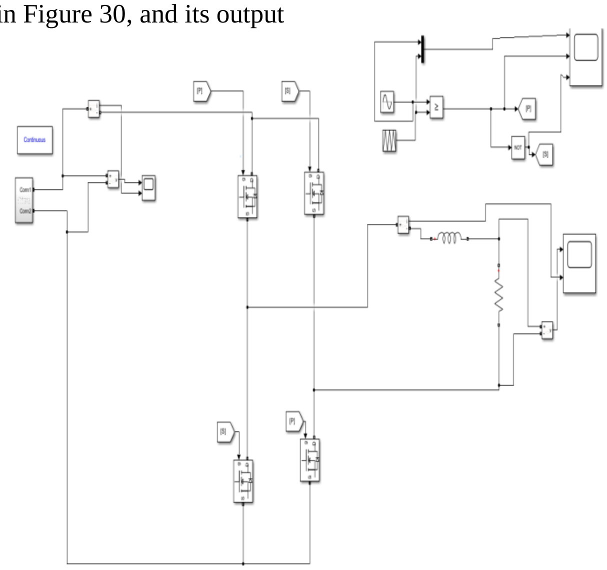

Fig. 30 Simulation Diagram of HGCDCC using Ultracapacitor as a Source

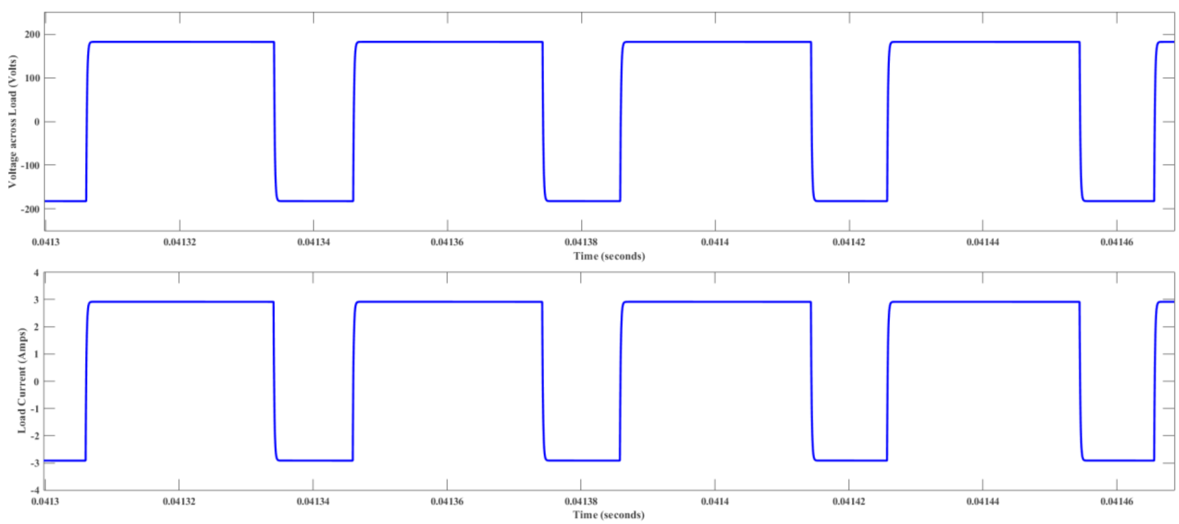

Fig. 31 Output Voltage and Output current of the IH load

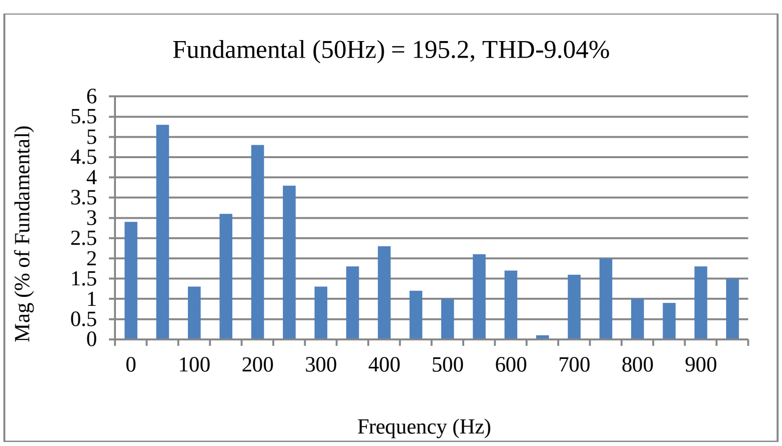

Fig. 32 Load voltage's THD using Ultracapacitor

3.3.3. UHGDCC

A single input source with two switches obtains an output voltage of high gain. The simulation circuit of UHGDCC is shown in Figure 33. The gate signals for switches with a duty ratio of 40%, which are turned ON for 40% of the time period and are in the OFF state, are depicted in Figure 34. From input and output voltages as well as output current, the gain of the topology can be found from Figure 35, which shows that the input voltage is 48V and the output voltage is 485V, as well as the output current is 4.85A.

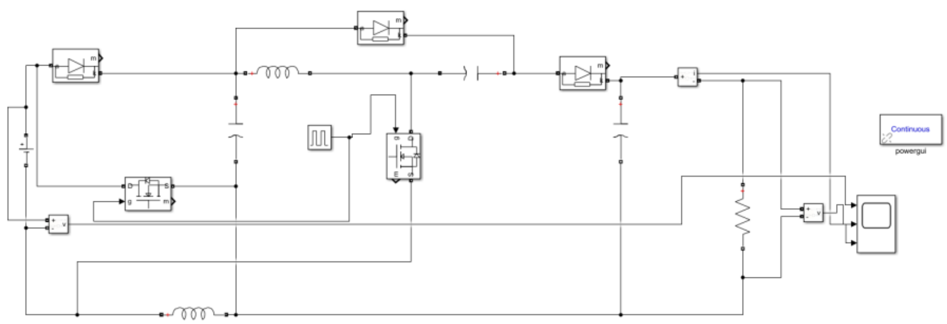

Fig. 33 Simulation Diagram of UHGDCC

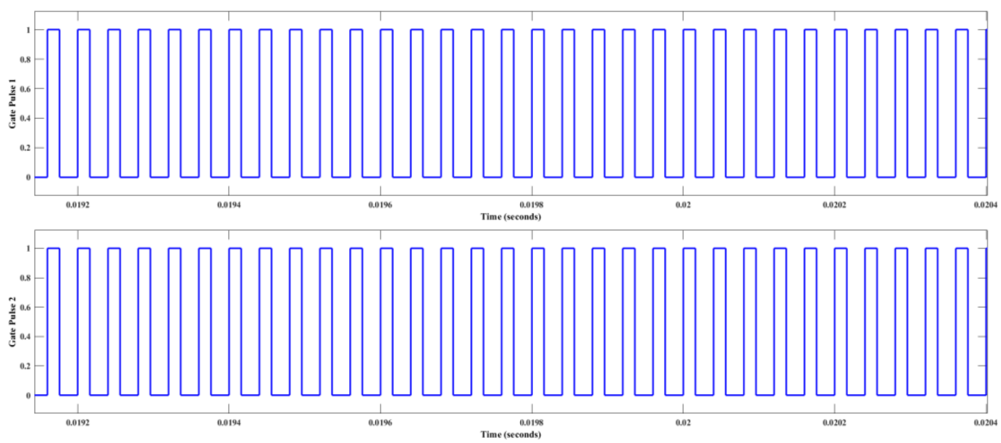

Fig. 34 Gate pulse for switches

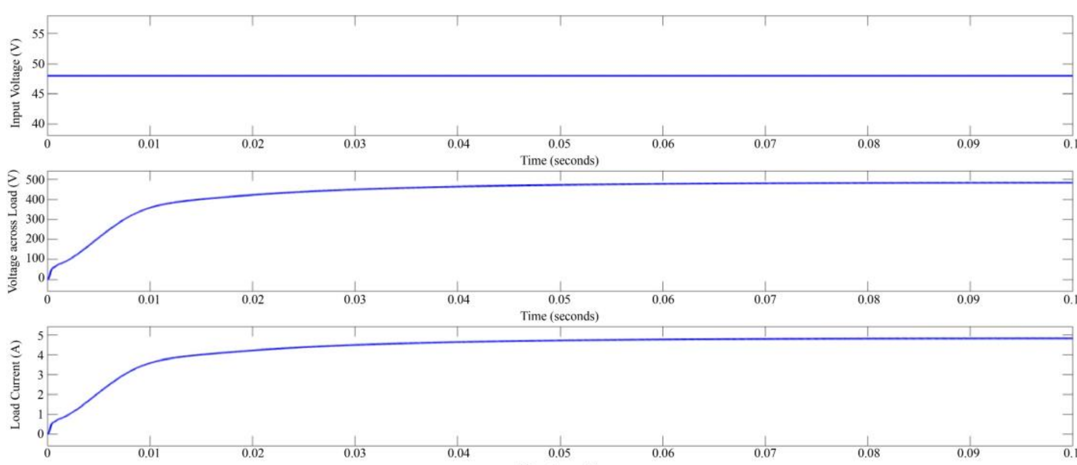

Fig. 35 Input Voltage, Output Voltage, and Load Current

3.3.4. UHGDCC using DC as a source

In the case of UHGDCC for IH load using DC voltage source, figure 36 represents the simulation circuit, figure 37 represents the IH output voltage and output current, and figure 38 represents the load voltage's THD.

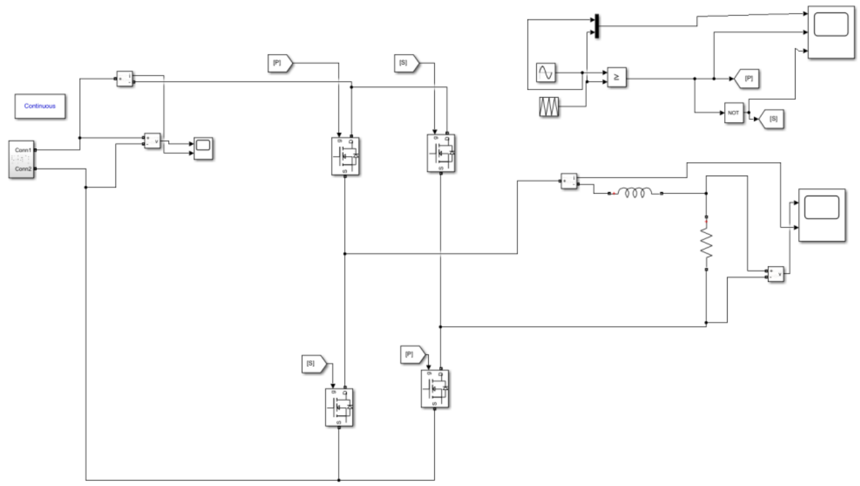

Fig. 36 Simulation Diagram of UHGDCC using DC Source

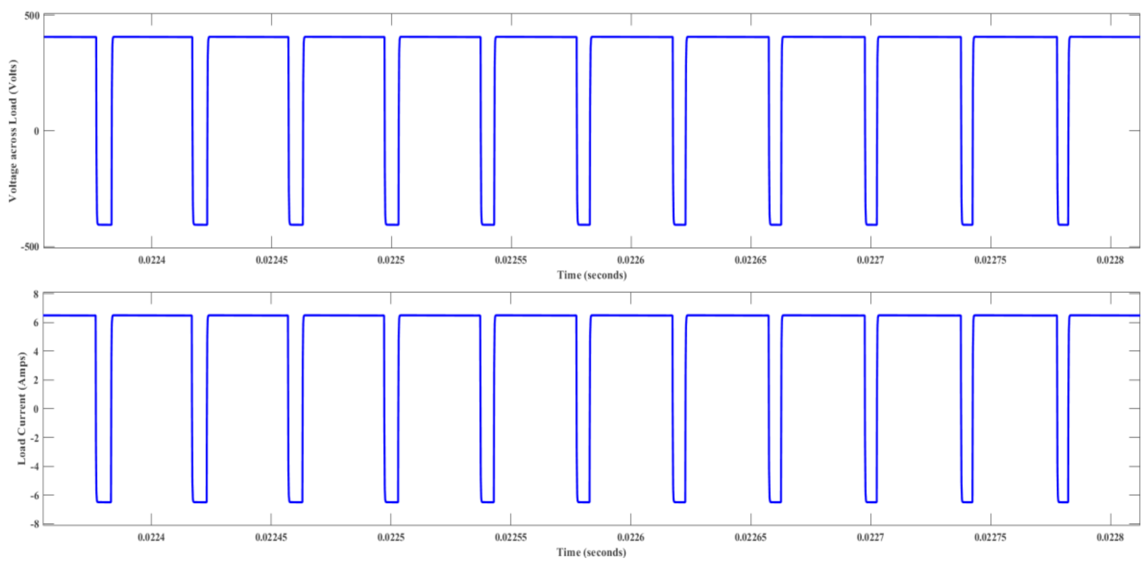

Fig. 37 Output Voltage and Output current of the IH load

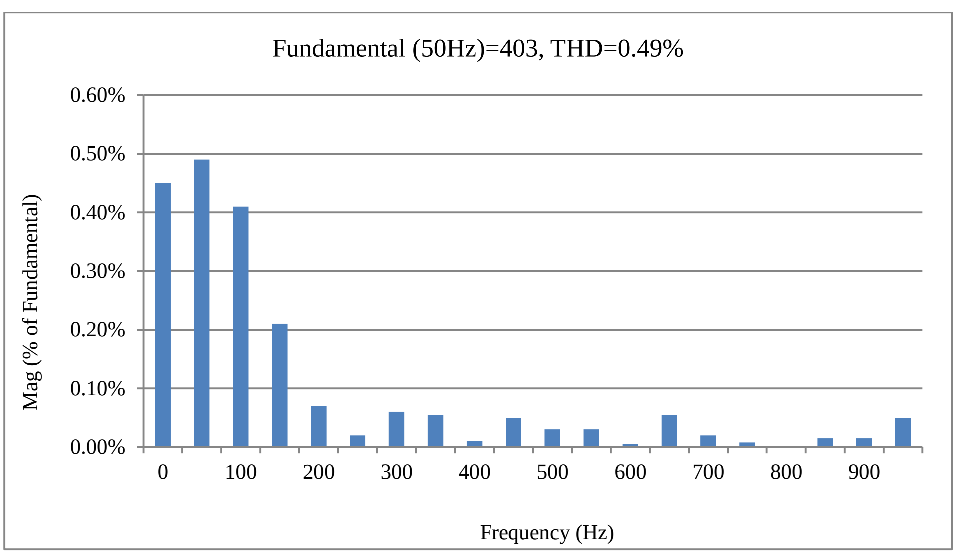

Fig. 38 Load voltage's THD using DC Voltage source

3.3.5. UHGDCC using Battery as a source

In the case of UHGDCC for IH load using Battery, Figure 39 tells us about the simulation diagram, and Figure 40 tells us about the output voltage and output current of the IH load. THD of load voltage is shown in Figure 41.

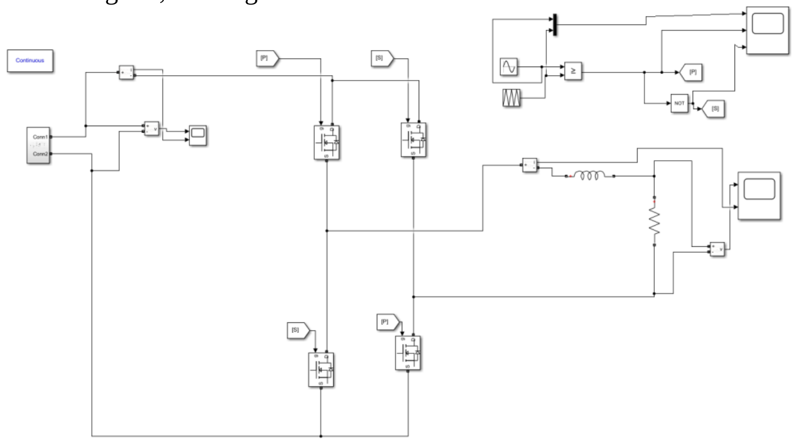

Fig. 39 Simulation Diagram of UHGDCC using Battery as a Source

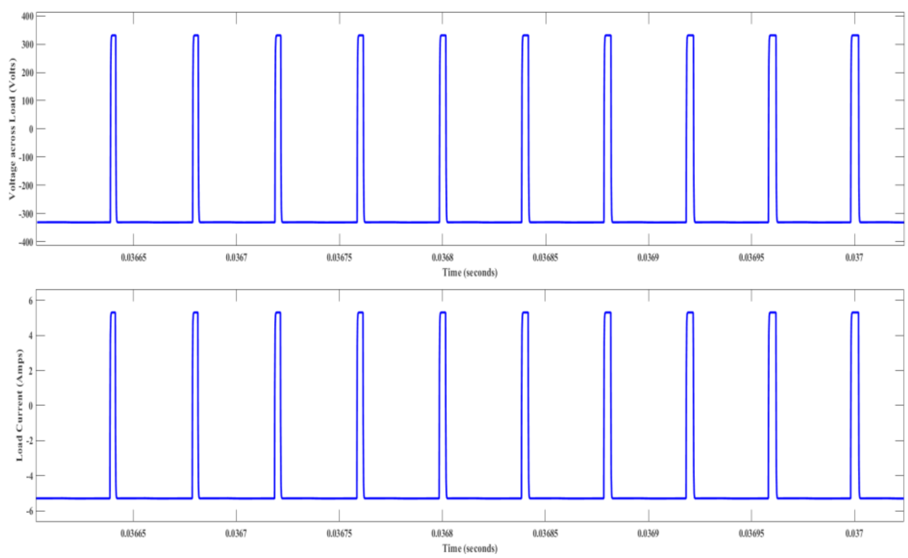

Fig. 40 Output Voltage and Output current of IH load

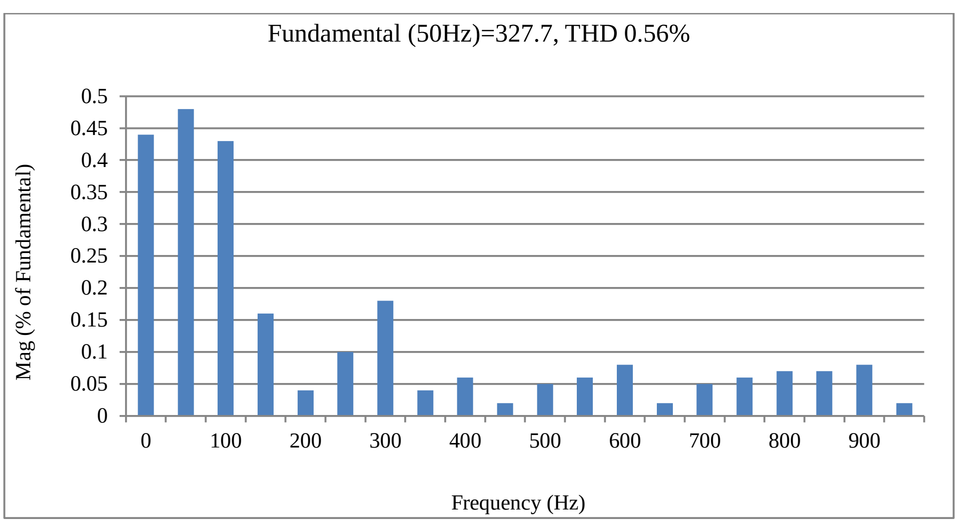

Fig. 41 Load voltage's THD using Battery

3.3.6. UHGDCC using Ultracapacitor as a source:

In the case of UHGDCC for IH load, using the Ultracapacitor simulation circuit is depicted in Figure 42, and its output voltage and output current of IH load are plotted in Figure 43. THD of load voltage is discussed in Figure 44.

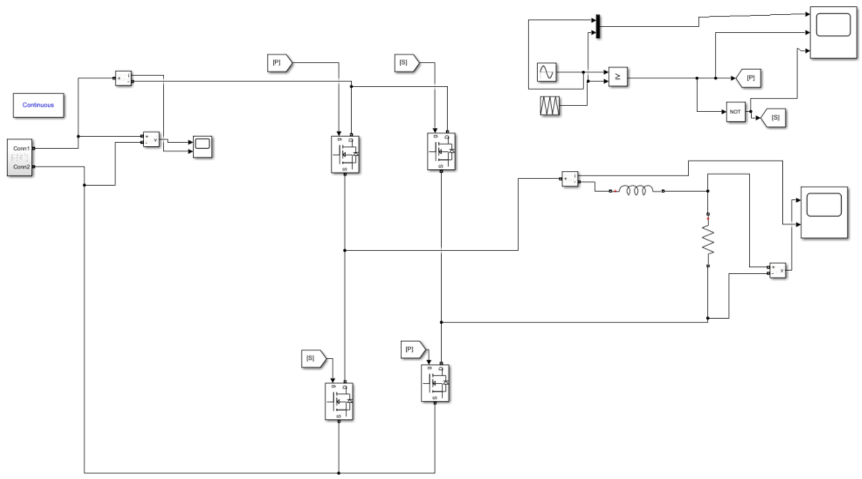

Fig. 42 Simulation Diagram of UHGDCC using Ultracapacitor as a Source

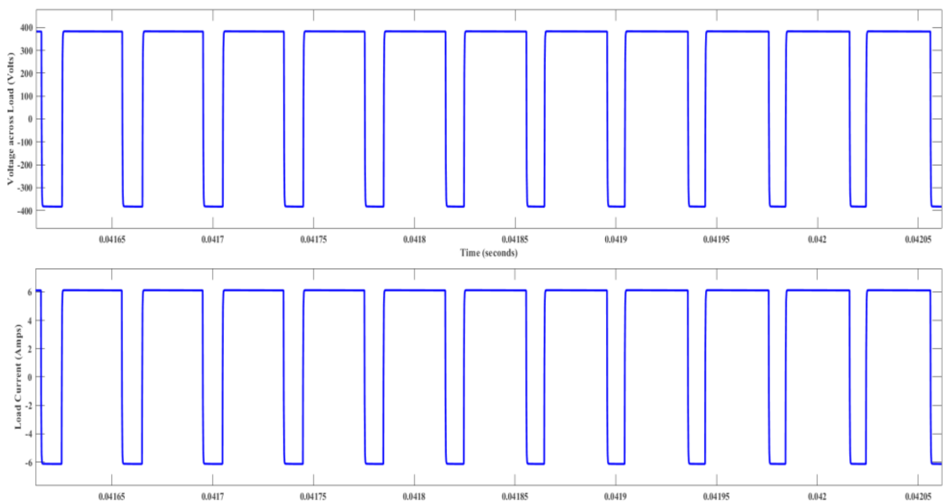

Fig. 43 Output Voltage and Output Current of IH load

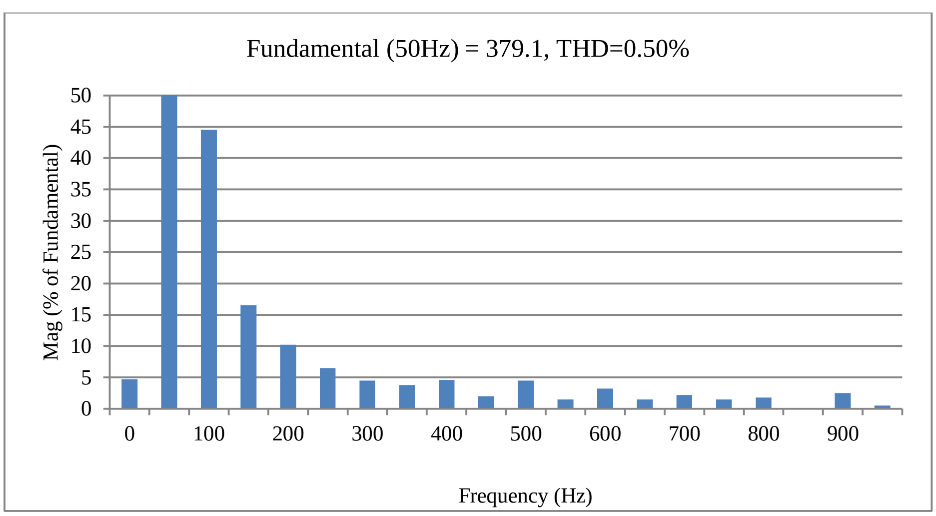

Fig. 44 Load voltage's THD using Ultracapacitor

Table 5 depicts the input, output, and gain of various topologies used in this work. Moreover, Table 6 represents THD of various topologies using various sources of energy like DC source, Battery, and Ultracapacitor when extended to IH application. Table 7 gives a comparison of existing topologies with the topologies utilized here in terms of gain and THD.

Table 5. Gain Of HGDCC, HGCDCC, UHGDCC

Topology	Input Voltage (V)	Output Voltage (V)	Gain
HGDCC	48	90	1.87
HGCDCC	48	210	4.37
UHGDCC	48	485	10.1

Table 6. %THD for HGDCC, HGCDCC, UHGDCC using various sources of energy

Topology	% THD using DC source	% THD using Battery	% THD using Ultracapacitor
HGDCC	6.36	6.37	9.41
HGCDCC	7	16.66	9.04
UHGDCC	0.49	0.56	0.50

Table 7. Gain, %THD of UHGDCC and HGDCDCC

Topology	Gain	% THD
UHGDCC	10	0.49
HGDCDCC [4]	5	0.38

4. Conclusion

High-Gain DC-DC Converter, High-Gain Cell DC-DC Converter, and Ultra High-Gain DC-DC converters are implemented using the MATLAB/SIMULINK environment. The proposed ultra-high gain DC-DC converter has a suitable high gain and uses fewer components than a high-gain cell converter topology.

The gain of the topologies was increased from 1.87 to 10.1. Furthermore, these converters' THD is found to be minimized from 9.41% to 0.50% of various converter topologies by using various sources of energy. And also, it can be concluded that with a smaller number of devices, the gain is improved and harmonics are minimized when compared with the existing topologies.

References

[1] Jagadeesh Ingilala, and Indragandhi Vairavasundaram "Investigation of High Gain DC/DC Converter for Solar PV Applications," *e-Prime - Advances in Electrical Engineering, Electronics and Energy*, vol. 5, pp. 1-12, 2023. [CrossRef] [Google Scholar] [Publisher Link]

[2] Z. M. Salem Elbarbary et al., "High Gain Chopper Supplied from PV System to Fed Synchronous Reluctance Motor Drive for Pumping Water Application," *Scientifc Reports*, vol. 12, pp. 1-15, 2022. [CrossRef] [Google Scholar] [Publisher Link]

[3] Chang-Hua Lin et al., "Design and Analysis of Novel High-Gain Boost Converter for Renewable Energy Systems (RES)," *IEEE Access*, vol. 12, pp. 24262-24273, 2024. [CrossRef] [Google Scholar] [Publisher Link]

[4] B. Harshini et al., "DC-DC Converter with High Gain Topology for Induction Heating Application," *2024 4th International Conference on Emerging Frontiers in Electrical and Electronic Technologies (ICEFEET)*, Patna, India, pp. 1-5, 2024. [CrossRef] [Google Scholar] [Publisher Link]

[5] Mohammad Ashar, "Integration of Ultra Capacitor with Battery using DC-DC Bidirectional Buck Boost Converter in an Electric Vehicle," *International Research Journal of Engineering and Technology*, vol. 3, no. 2, pp. 1-5, 2016. [Google Scholar] [Publisher Link]

[6] A. Lavanya et al., "Selection of Renewable Energy Materials for Dual Input DC–DC Converter Based Hybrid Energy System," *Materials Today: Proceedings*, vol. 34, no. 2, pp. 379-385, 2021. [CrossRef] [Google Scholar] [Publisher Link]

[7] Arafa S. Mansour, and Mohamed S. Zaky, "A New Extended Single-Switch High Gain DC–DC Boost Converter for Renewable Energy Applications," *Scientific Reports*, vol. 13, pp. 1-22, 2023. [CrossRef] [Google Scholar] [Publisher Link]

[8] Nikolay Madzharov, and Nikolay Hinov, "Analysis and Design of Resonant DC/AC Converters with Energy Dosing for Induction Heating," *Energies*, vol. 16, no. 3, pp. 1-16, 2023. [CrossRef] [Google Scholar] [Publisher Link]

[9] R. Subbulakshmy et al., "Implementation of Non-Isolated High Gain Interleaved DC-DC Converter for Fuel Cell Electric Vehicle Using ANN-Based MPPT Controller," *Sustainability*, vol. 16, no. 3, pp. 1-26, 2024. [CrossRef] [Google Scholar] [Publisher Link]

[10] Jayanthi Kathiresan, and Gnanavadivel Jothimani, "High Gain Converter Design and Implementation for Electric Vehicles," *International Journal of Electrical and Electronics Research*, vol. 10, no. 4, pp. 1058-1063, 2022. [CrossRef] [Google Scholar] [Publisher Link]

[11] Ramin Rahimi et al., "Z-Source-Based High Step-Up DC–DC Converters for Photovoltaic Applications," *IEEE Journal of Emerging and Selected Topics in Power Electronics*, vol. 10, no. 4, pp. 4783-4796, 2022. [CrossRef] [Google Scholar] [Publisher Link]

[12] Ahmed Allehyani, "Analysis of A Transformerless Single Switch High Gain DC–DC Converter for Renewable Energy Systems," *Arabian Journal for Science and Engineering*, vol. 46, pp. 9691-9702, 2021. [CrossRef] [Google Scholar] [Publisher Link]

[13] Vinay Rathore et al., "A High-Gain Multilevel dc–dc Converter for Interfacing Electric Vehicle Battery and Inverter," *IEEE Transactions on Industry Applications*, vol. 58, no. 5, pp. 6506-6518, 2022. [CrossRef] [Google Scholar] [Publisher Link]

[14] R. Rakhee, and M.G. Shelma, "High Gain Direct AC-AC Resonant Converter Applied to Domestic Induction Heating Applications," *International Journal of Advanced Research in Electrical, Electronics and Instrumentation Engineering*, vol. 5, pp. 1-6, 2016. [Publisher Link]

[15] Rini Paul, P. Ramesh Kumar, and A. Amar Dutt, "A High Gain Step Up Z-Source DC-DC Converter Feeding a Multilevel Inverter," *2017 IEEE Region 10 Symposium (TENSYMP)*, Cochin, India, pp. 1-5, 2017. [CrossRef] [Google Scholar] [Publisher Link]

[16] K.P. Swaroop et al., "Ultra-Gain DC-DC Converter fed 3-Φ Inverter for Variable-Speed Drive Applications," *2023 IEEE 3rd International Conference on Smart Technologies for Power, Energy and Control (STPEC)*, Bhubaneswar, India, pp. 1-6, 2023. [CrossRef] [Google Scholar] [Publisher Link]

[17] Qingxin Tian et al., "Ultra-High-Voltage Gain DC–DC Converter Based on Three-Winding Coupled Inductor with Ripple Free Input Current and Soft Switching for Renewable Energy Applications," *IEEE Transactions On Power Electronics*, vol. 40, no. 9, pp. 13686-13702, 2025. [CrossRef] [Google Scholar] [Publisher Link]

[18] Hanan H. Kawshty, Khairy Sayed, and Ahmed Elnozahy, "Design and Analysis of High Frequency Inverter for Induction Heating Application," *2023 24th International Middle East Power System Conference (MEPCON)*, Mansoura, Egypt, pp. 1-8, 2023. [CrossRef] [Google Scholar] [Publisher Link]

[19] Porselvi Thandavarayan, and Arounassalame Mouttou, "A Novel High-Gain DC-DC Converter for Photovoltaic Applications," *Bulletin of Electrical Engineering and Informatics*, vol. 13, no. 6, pp. 3919-3927, 2024. [CrossRef] [Google Scholar] [Publisher Link]